3 Results

3.1 Generation of expression and targeting vectors

3.1.1 ChAT-GFP and wildtype ChAT expression vectors

In order to test the functionality of a ChAT-GFP fusion protein and to compare its properties with the wildtype enzyme the mouse ChAT cDNA was cloned. The 1923 bp cDNA sequence comprising the entire coding region was isolated by reverse transcription of total RNA prepared from the spinal cord of C57Bl/6 mice and subsequent PCR amplification with the primer pair "JRChATfor/JRChATamp9" deduced from the published ChAT sequence (Ishii *et al*., 1990). The wildtype ChAT expression vector *pJR33* was obtained by cloning the ChAT cDNA into the EcoRI site of the *pRK5* expression vector under the control of the cytomegalovirus (CMV) promoter. The enhanced, red-shifted EGFP cDNA sequence with humanized codon usage for improved expression in mammalian systems (Zolotukhin *et al*., 1996) was amplified by PCR from the plasmid vector *pTR-UF2* with the primer pair "hGFPHIIIfor/rev" and inserted in frame into the unique HindIII site 48 bp downstream of the start codon of the ChAT cDNA. At the 5´-HindIII restriction site a frameshift mutation had been generated which was corrected by site-directed mutagenesis with the primer pair Mut-JR14.for/rev. The 3´-HindIII restriction site "AAGCTT" of the GFP sequence is flanked in the ChAT-GFP sequence by "AAGC" resulting in "AAGCAAGCTT". Digestion with HindIII and ligation of the GFP-HindIII fragment into the ChAT sequence led to a frameshift mutation by the loss of "AAGC" and required site-directed mutagenesis for correction (primer pair "Mut-ChATGFP.for/rev"). This finally resulted in the ChAT-GFP expression vector *pJR38*. Both expression constructs pRK5-ChAT (*pJR33*) and pRK5-ChAT-GFP (*pJR38*) are shown in Figure 3.1.

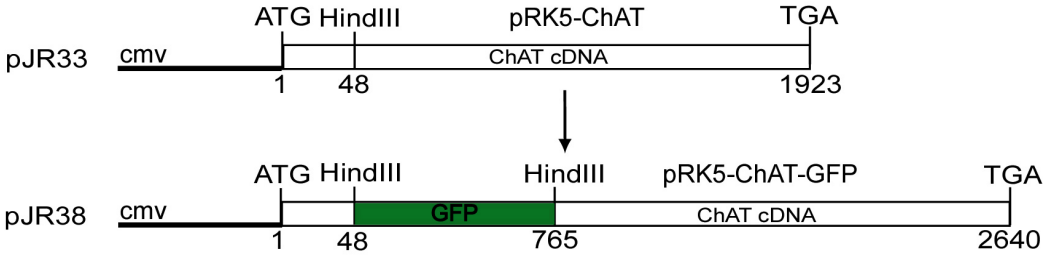

Fig. 3.1 Cloning of the wildtype ChAT and ChAT-GFP expression constructs. The ChAT cDNA was isolated by RT-PCR from mouse spinal cord and cloned into *pRK5* resulting in pRK5-ChAT (*pJR33*). The GFP sequence was inserted into the unique HindIII site to obtain pRK5-ChAT-GFP (*pJR38*). cmv, cytomegalovirus promoter.

3.1.2 ChAT-GFP targeting vector

The genomic clones λChAT4-1 and λChAT4-2 containing parts of the ChAT gene were isolated by Dr. M. Koenen from a 129 mouse genomic library and flanking regions of exon 2 were identified, sequenced and subcloned into the *pBKS* plasmid vector to get a XhoI-XbaI-fragment comprising 5.8 kb of the promoter region (*p958*) and a 3 kb XbaI-XbaI-fragment harbouring exon 2 (*p974/2*). These were provided by Dr. Michael Koenen. By site-directed mutagenesis using the primers "Mut-SalI.for/rev" a SalI site was introduced into *p974/2* 150 bp behind exon 2 to obtain *pJR5*. Then a NotI site was introduced with the primers "Mut-NotI.for/rev" 1500 bp downstream of exon 2 (*pJR10*) and from this clone an EcoRI-NotI-fragment was subcloned into the *p1029* vector (*pJR18*). The PpuMI-HindIII-fragment of *pJR38* (see Section 3.1.1) was introduced into *pJR18*, which resulted in *pJR20*. Due to this HindIII restriction a 650 bp HindIII fragment was excised which had subsequently been cloned back (*pJR22*). Digestion with HindIII also led to the deletion of four base pairs (AAGC) adjacent to the 5´-HindIII site of the GFP sequence evoking a frameshift mutation (see Section 3.1.1). Mutagenesis of *pJR22* with the primers "Mut-ChATGFP.for/rev" yielded *pJR45*. The 5.8 kb XhoI-XbaI-promoter fragment of *p958* was cloned into *pJR45* to obtain *pJR46*. Finally the XhoI fragment of the "floxed" neo^r cassette of the plasmid *ploxneo3.repair* was inserted into the SalI site providing the ChAT-GFP targeting vector *pJR48*. The most important cloning steps are summarized in Figure 3.2.

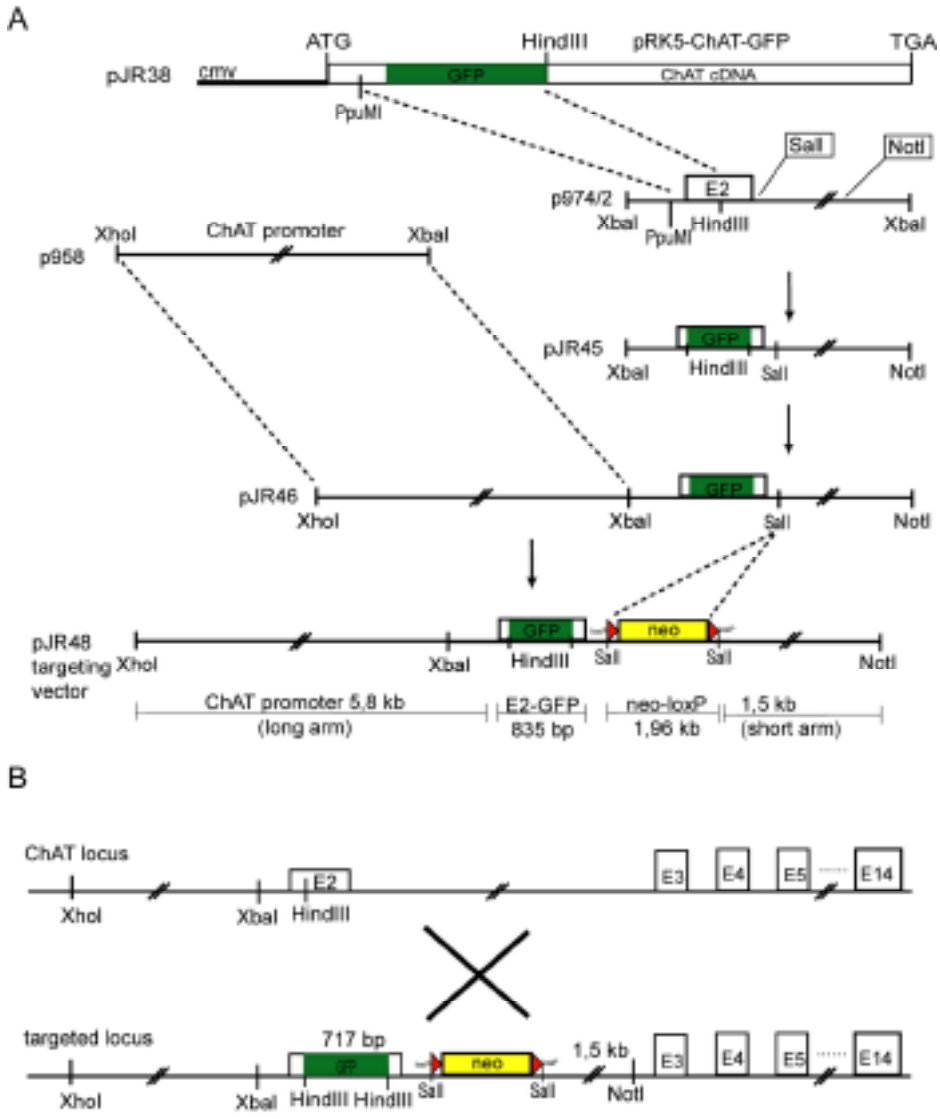

Fig. 3.2 Cloning strategy of ChAT-GFP targeting vector and homologous recombination of the ChAT genomic locus. A) A SalI and a NotI stite was introduced into the precursor clone *p974/2*. The GFP sequence was cloned from *pJR38* as a PpuMI-HindIII fragment. The promoter sequence was cloned from *p958* as XhoI-XbaI fragment. Finally the loxP-neo^r-loxP sequence was cloned to obtain the targeting vector *pJR48*. B) Homologous recombination between the ChAT locus and the targeting vector *pJR48* resulted in the ChAT-GFP targeted locus.

Each cloning step was confirmed by restriction digestion and DNA sequence analysis. The targeting vector was linearized by XhoI digestion and electroporated into E14-1 embryonic stem cells for homologous recombination.

3.1.3 ChAT-loxP targeting vector

A BglII site was introduced between the 5´splice site and the start ATG of exon 2 by site-directed mutagenesis of *pJR18* (see Section 3.1.2) with the primer pair "JR18MutBglIIfor/rev" (*pJR49*). The 34 bp loxP site, consisting of the 55 bp long complementary oligonucleotides "JRloxPfor/rev" equipped with overhanging BglII sites, was ligated into this BglII site providing *pJR51*. The 5.8 kb XhoI-XbaI-promoter fragment of *p958* was cloned into *pJR51* to obtain *pJR52*. The neo^r cassette with one loxP site at the 3´-end was amplified by PCR using the primers "NeoSalloxPfor/rev" from the plasmid *ploxneo3.repair* and ligated into the SalI site downstream of exon 2 which resulted in the final ChAT-loxP targeting vector *pJR54*. The most important steps of the cloning strategy are shown in Figure 3.3.

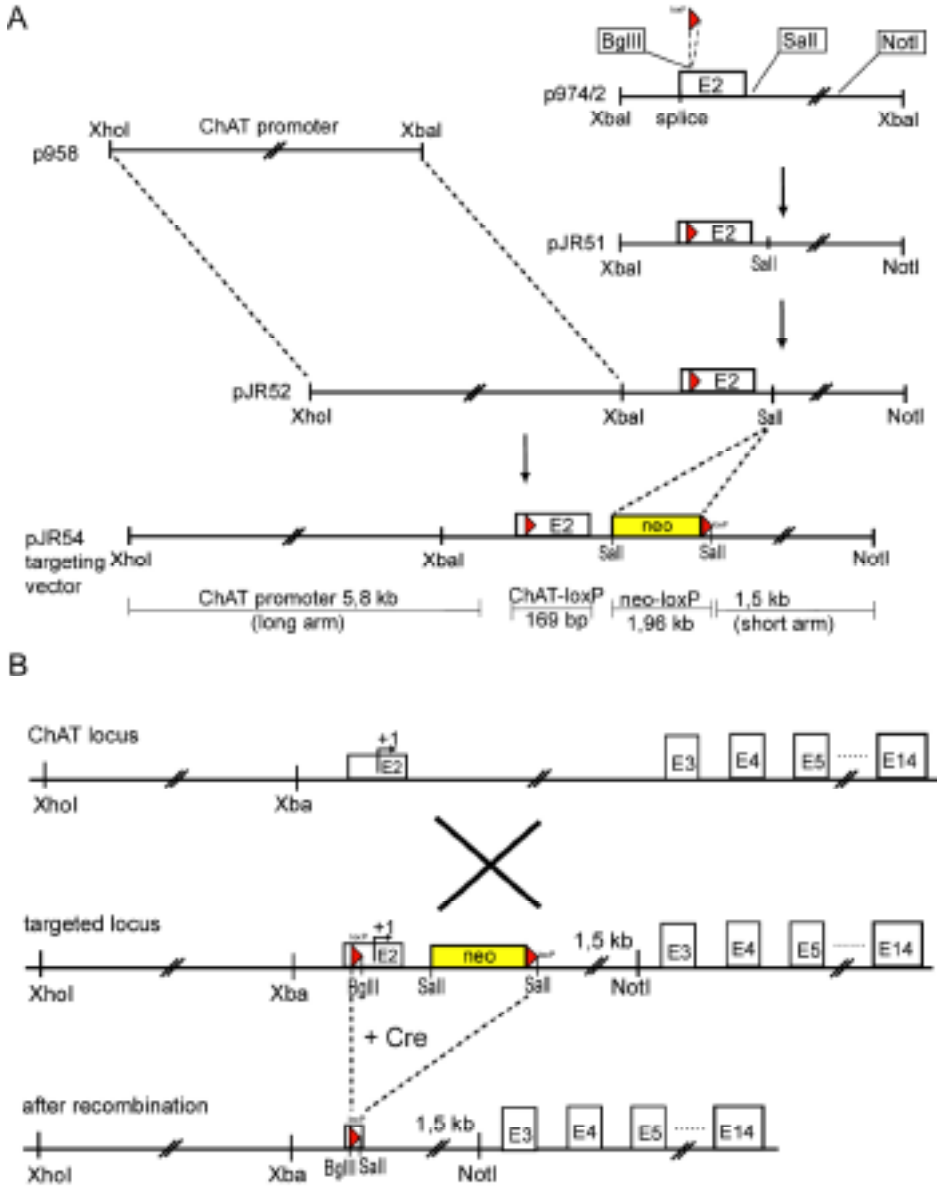

Fig. 3.3 Cloning strategy of the ChAT-loxP targeting vector and homologous recombination of the genomic locus. A) A BglII, a SalI and a NotI stite was introduced into the precursor clone *p974/2*. The loxP sequence was cloned into the BglII site. The promoter sequence was cloned from *p958* as XhoI-XbaI fragment. Finally the neo^r-loxP sequence was cloned to obtain the targeting vector *pJR54*. B) Homologous recombination between the ChAT locus and the targeting vector *pJR54* resulted in the ChAT-loxP targeted locus.

Each cloning step was confirmed by restriction digestion and DNA sequence analysis.

To verify that both loxP sites are functional, the ChAT-loxP (*pJR54*) targeting vector was transformed into the Cre recombinase expressing bacteria strain BS591

which led to the excision of the loxP flanked 2.2 kb fragment containing the coding region of exon 2 and the neo^r cassette. The HpaI/NotI fragment of *pJR54* obtained from the BS591 strain was reduced from about 4.2 kb to 2 kb as shown in Figure 3.4.

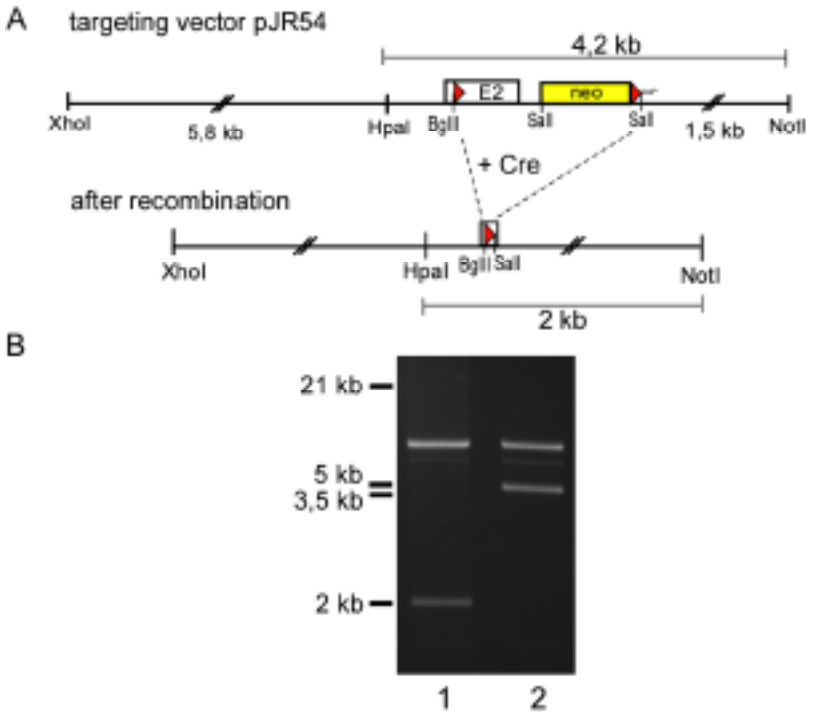

Fig. 3.4 Cre-mediated recombination of targeting vector *pJR54*. The targeting vector was transformed into Cre recombinase-expressing bacteria to confirm that both loxP sites are functional. A) Schematic representation of *pJR54* before and after recombination. The "floxed" 2.2 kb fragment comprising exon 2 and the neo^r cassette is excised by Cre-mediated recombination. B) The plasmid DNA of *pJR54* prepared from BS591 (lane 1) and *pJR54* prepared from HB101 (lane 2) was digested with HpaI and NotI and analyzed by agarose gel electrophoresis. Lane 1 shows the reduced HpaI/NotI fragment of 2 kb, lane 2 shows the original HpaI/NotI fragment of 4.2 kb.

The targeting vector was linearized by XhoI digestion and electroporated into E14-1 embryonic stem cells for homologous recombination.

3.2 Functional characterization of the ChAT-GFP fusion protein

3.2.1 Expression of ChAT-GFP and wildtype ChAT

Expression studies were performed in COS-1 cells since they do not express endogenous ChAT. Western blot analysis confirmed that the protein was expressed in COS-1 cells which were transiently transfected with the expression constructs pRK5-ChAT (*pJR33*), pRK5-ChAT-GFP (*pJR38*) and *pRK5* as vector control. The cells were lysed 48 h after transfection (see Section 2.2.2.1). Proteins were separated by SDS-PAGE (Fig. 3.5A) and transferred to PVDF membrane. The membrane was probed with polyclonal affinity purified anti-ChAT antibody AB144P, detecting both wildtype ChAT as well as the ChAT-GFP fusion protein. The Mr of the wildtype ChAT protein of 71.7 kDa (Fig. 3.5B, lane 4, open arrowhead) was shifted to 98.6 kDa when fused to GFP (Fig. 3.5B, lane 5, filled arrowhead). The antibodies were removed from the membrane, which was then incubated with monoclonal anti-GFP antibody IL-8. Only the ChAT-GFP signal of 98.6 kDa was confirmed (Fig. 3.5C, lane 8) while the wildtype ChAT protein was not detected (Fig. 3.5C, lane 7). No signal appeared in the control transfection (Fig. 3.5B, lane 6; 3.5C, lane 9). The results indicated that recombinant wildtype mouse ChAT and ChAT-GFP fusion protein were efficiently expressed in COS-1 cells. In the case of the polyclonal anti-ChAT antibody stain cross-reactivity occurred which was not seen for the monoclonal anti-GFP antibody. ChAT-GFP appeared to be rather stable against proteolysis since no degradation could be detected.

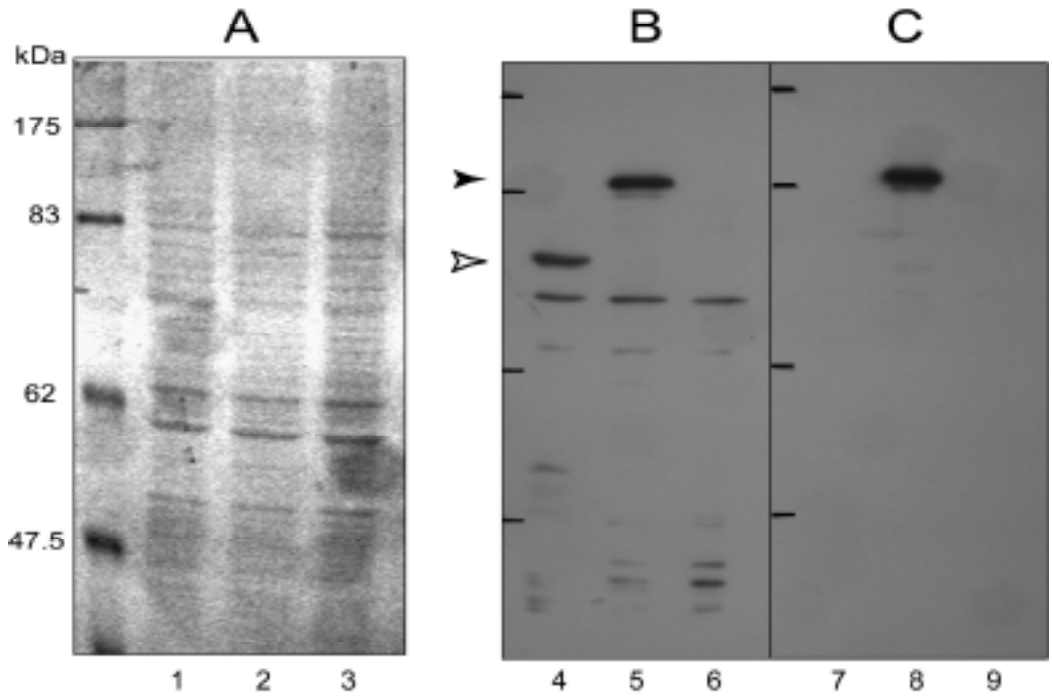

Fig. 3.5 Western blot analysis of recombinant ChAT-GFP and wildtype ChAT. COS-1 cells were harvested 2 days after transfection and lysed. Proteins were analysed by 10 % SDS-PAGE (lane 1, 4, 7 transfection with *pRK5-ChAT*/ lane 2, 5, 8 transfection with *pRK5-ChAT-GFP*/ lane 3, 6, 9 transfection with *pRK5*). A) Coomassie Blue stained gel shows that similar amounts of protein (20 µg) had been applied to each lane. Left lane: prestained marker proteins, Mr as indicated. B) The gel was blotted onto a PVDF membrane which was probed with an anti-ChAT-antibody. Open arrowhead indicates wildtype ChAT (Mr 71.7), filled arrowhead ChAT-GFP (Mr 98.6). The control in lane 6 reveals a number of additional bands, which are probably due to nonspecific cross reactivity of this antibody against ChAT. C) Antibodies were removed from the blot in B which was then incubated with anti-GFP-antibody. Black bars in B and C are Mr as in A. The fusion protein ChAT-GFP in lane 8 revealed no detectable degradation products.

3.2.2 Enzyme activity of ChAT-GFP compared to the wildtype enzyme

To determine whether insertion of GFP into the N-terminal sequence affects the enzyme activity of ChAT, COS-1 cells were transfected with pRK5-ChAT (*pJR33*), pRK5-ChAT-GFP (*pJR38*) and *pRK5* as vector control. The ChAT activity was assayed 48 hours following the transfection by using a radiochemical assay (Fonnum, 1975). COS-1 cells which were expressing wildtype ChAT or ChAT-GFP were lysed (see

Section 2.2.2.1) and the crude cell lysates were assayed for the ability to synthesize tritium labeled acetylcholine from ^{3}H-acetyl-CoA and choline.

Prior to the enzyme assay, the protein concentrations of the lysates were determined. The wildtype enzyme showed a specific activity of 19 nmol/h/mg protein while the activity of ChAT-GFP was 14 nmol/h/mg (Table 1). Assuming that the transfection efficiencies of wildtype ChAT and ChAT-GFP were similar, enzyme activities of the cell lysates can be compared, even when the ChAT proteins were not further purified.

Tab. 3.1 ChAT enzyme activity of COS-1 cell lysates.

	pRK5-ChAT	pRK5-ChAT-GFP	pRK5
specific activity (nmol/h/mg)	19.08 ± 2.76	14.04 ± 0.156	0.36 ± 0.006

COS-1 cells were transfected with respective expression vectors. Enzyme activity measurements were performed in duplicates and values were calculated from three independent experiments according to the method of Fonnum (1975).

The reduction of the enzyme activity of ChAT-GFP by about 27 % compared to the wildtype ChAT may be due to the insertion of the relatively large GFP sequence into the sequence of ChAT. Nevertheless, 73 % of the enzyme activity is still present and will produce sufficient acetylcholine in the GFP targeted animals.

3.2.3 Subcellular distribution of ChAT-GFP and wildtype ChAT in COS-1 cells

To see whether GFP changes the subcellular localization of the ChAT protein, the distribution of ChAT-GFP and wildtype ChAT in COS-1 cells was analyzed. The cells transfected with pRK5-ChAT (*pJR33*) and *pRK5* were fixed 48 hours after transfection (see Section 2.2.2.6) and stained for the expression of ChAT using the polyclonal affinity purified anti-ChAT antibody AB144P and a FITC-labeled secondary antibody. Cells transfected with pRK5-ChAT-GFP (*pJR38*) and *pTU-UF2* (GFP) were fixed and mounted immediately. Single sections of confocal images display the expression of wildtype ChAT and ChAT-GFP (Figure 3.6A, A´, A´´ and 3.6B, B´, B´´). The similar subcellular distribution of both transgenic proteins is demonstrated by

images of three individual cells. Here, wildtype ChAT as well as the ChAT-GFP fusion protein were located in the cytoplasm and were absent from the nucleus. Two images of individual cells expressing GFP demonstrate that this protein was distributed uniformly throughout the cytoplasm and nucleus (Figure 3.6C, C´) as shown previously by Ogawa *et al*. (1995). Cells transfected with pRK5 showed no staining apart from a very low background signal supporting the notion that COS-1 cells contain no endogenous ChAT (Figure 3.6D).

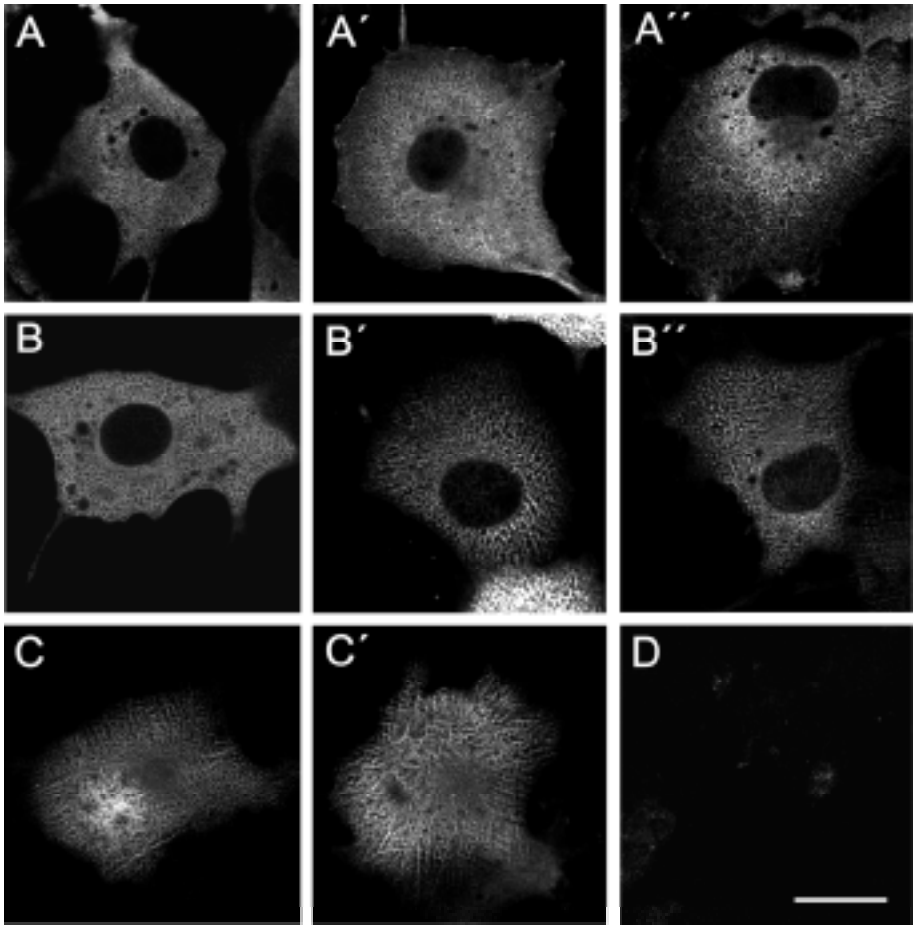

Fig. 3.6 Distribution of recombinant ChAT-GFP, GFP and wildtype ChAT in COS-1 cells. COS-1 cells were plated on coverslips, transfected with pRK5-ChAT, pRK5-ChAT-GFP, pRK5-GFP and pRK5 and fixed 48 hours after transfection. The confocal images represent single sections. A, A´, A´´) Expression of ChAT was visualized by immunostaining with anti-ChAT-antibodies and FITC-coupled rabbit anti-goat antibodies. B, B´, B´´) Expression of ChAT-GFP as observed by the green fluorescence of the fusion protein. C, C´) Expression of GFP (green fluorescence). D) Control cells were transfected with pRK5 and immunostained with anti-ChAT-antibodies and FITC-coupled rabbit anti-goat antibodies. Scale bar 20 µm.

3.2.4 Subcellular distribution of ChAT-GFP in hippocampal neurons

Primary cultures of hippocampal neurons were used to express the ChAT-GFP fusion protein to study its distribution and fluorescence in neurons (Rathenberg *et al.*, 2002). Imaging of the ChAT-GFP expressing neurons revealed both in live cells (Figure 3.7A) and after fixation (Figure 3.7B) that the fusion protein was distributed in the soma and neuritic processes (Figure 3.7a) and was absent from the nucleus (Figure 3.7b). There was no apparent difference in fluorescence intensities before and after the fixation procedure of primary neurons. The efficiency of transfection by the lipofection method was about 1-2 % of cells for primary cultures.

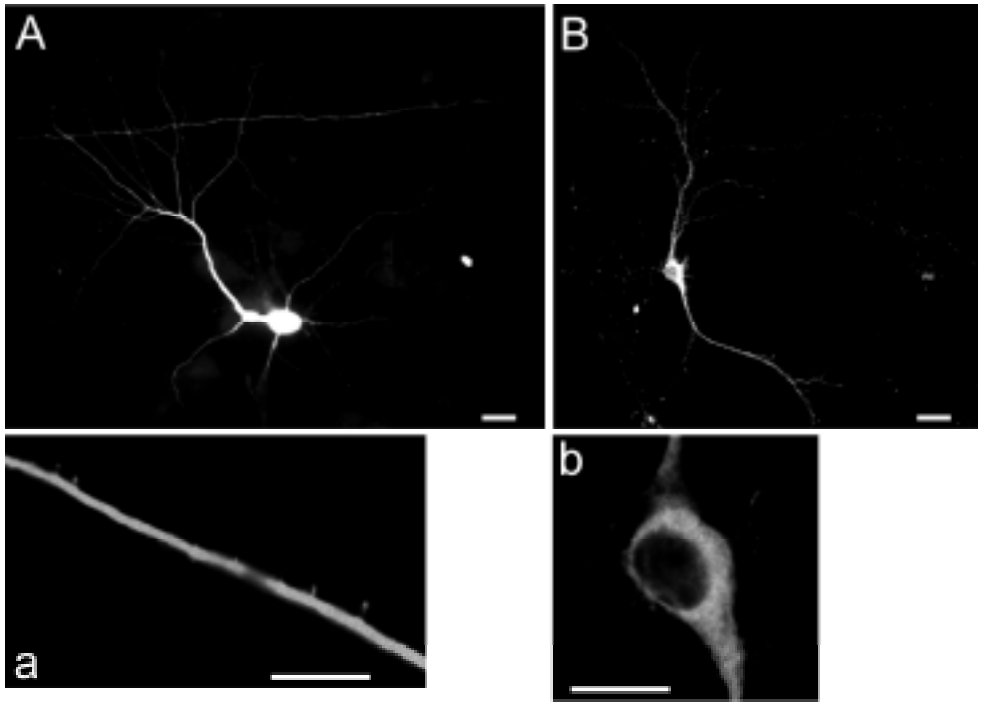

Fig. 3.7 Distribution of ChAT-GFP in hippocampal primary culture. Hippocampal neurons were prepared from E19 Wistar rat embryos, cultured on coverslips for 7 days and transfected with pRK5-ChAT-GFP (pJR38). Fluorescently labeled cells were imaged before fixation (A). For imaging by confocal microscopy the neurons were fixed (B). Images with higher magnification show a neurite of a living neuron (a) and the cell body of the neuron in B (b). Scale bars in A 10 µm and B 20 µm, in a and b 10 µm.

To complement these findings for primary cultures of hippocampal neurons single-cell electroporation SCE (see Section 3.3) was applied to analyze the distribution of ChAT-GFP in pyramidal neurons in organotypic hippocampal slice cultures where

the neuronal morphology is very well retained. The expression vectors for ChAT-GFP (*pJR38*) and GFP (*pEGFP-C1*) were electroporated into pyramidal neurons in the CA3 region of organotypic hippocampal brain slice cultures 6 days *in vitro* (see Section 2.2.4). Transgenic proteins were expressed in about 25-50 % of electroporated cells (after SCE has been optimized) and bright fluorescence could be observed about 12 hours after electroporation.

Fluorescence imaging of living neurons was performed 20 hours after electroporation. The slices were placed into oxygenated physiological salt solution during image acquisition. Images were acquired with a Zeiss AxioplanII fluorescence microscope with a 63x water immersion objective. ChAT-GFP was present in the axon (Figure 3.8a), dendritic spines (Figure 3.8a´) but not in the nucleus (Figure 3.8a´´) similar to the results gained from the primary cultures. GFP was present in the axon (Figure 3.8b), dendritic spines (Figure 3.8b´) and in the nucleus (Figure 3.8b´´). Direct comparison of the subcellular localization of ChAT-GFP and GFP was possible since the expression levels of the transgenic proteins in both cells were similar. ChAT-GFP translocated over long distances into axonal processes of area CA1 while GFP remained under the same conditions in axonal processes nearby the soma in CA3. Thus the distance between the soma and the imaged axonal part was higher for the ChAT-GFP expressing cell than for the GFP expressing cell. Axonal processes in CA1 could also be seen for GFP expressing cells but only after longer expression times or when expression levels were higher. The faster appearance of ChAT-GFP in axonal processes of CA1 could indicate that it is actively transported. The results gained from synaptophysin-GFP expressing cells are consistent with this hypothesis (see Section 3.4).

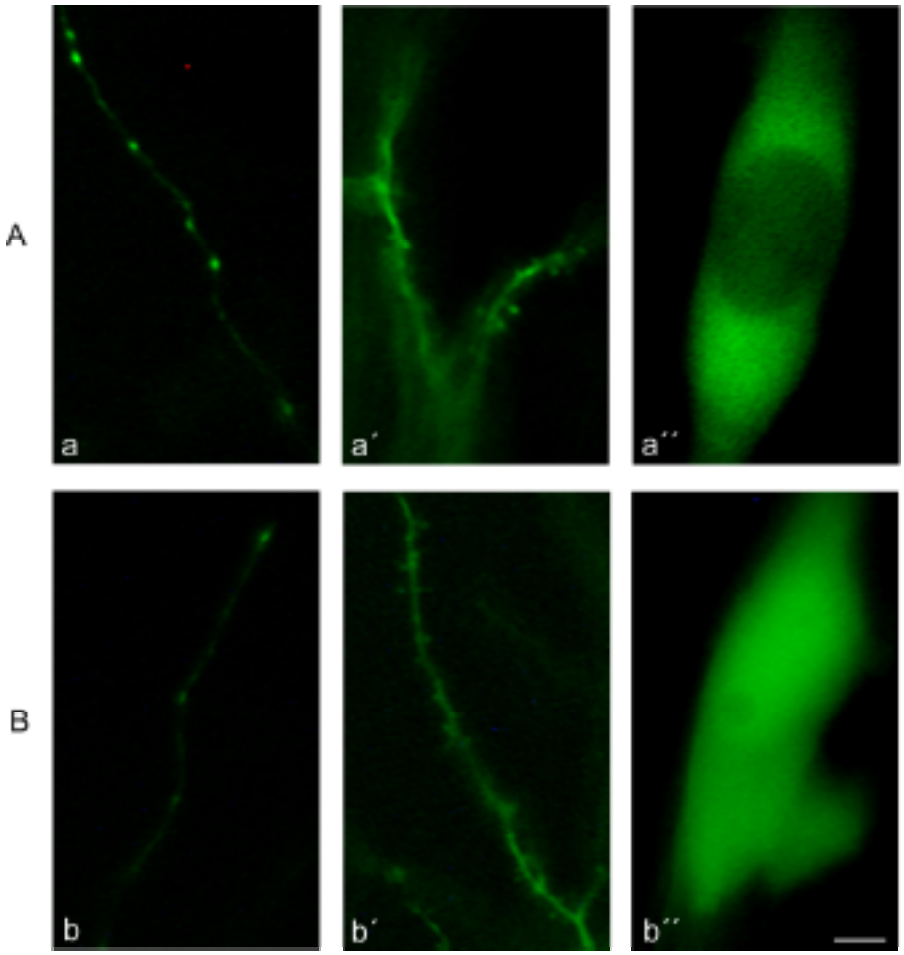

Fig. 3.8 Distribution of ChAT-GFP and GFP in CA3 hippocampal neurons of living organotypic brain slice culture. The plasmids *pJR38* (A) and *pEGFP-C1* (B) were electroporated into pyramidal neurons of CA3 of hippocampal slice cultures. The slices were imaged using a fluorescence microscope 20 hours after transfection. ChAT-GFP is present in the axon (a), dendritic spines (a´) and is absent from the nucleus (a´´). GFP is present in the axon (b), dendritic spines (b´) and the nucleus (b´´). Scale bar 5 µm.

For the visualization by confocal microscopy the slices were fixed. Maximum projections of stacks of single sections show that ChAT-GFP was distributed in the soma, translocated into the axon (Figure 3.9A, a) and was also present in the dendrites and spines at elevated levels (Figure 3.9a´). ChAT-GFP was transported along axonal processes to the CA1 area, as revealed by the bright fluorescence of the dense network of axonal varicosities (Figure 3.9a´´). Higher magnification of axonal terminals indicated an accumulation of ChAT-GFP fluorescence in presynaptic boutons (Figure 3.9a´´´). The distribution was very similar to that of synaptophysin-GFP (Figure 3.14a´

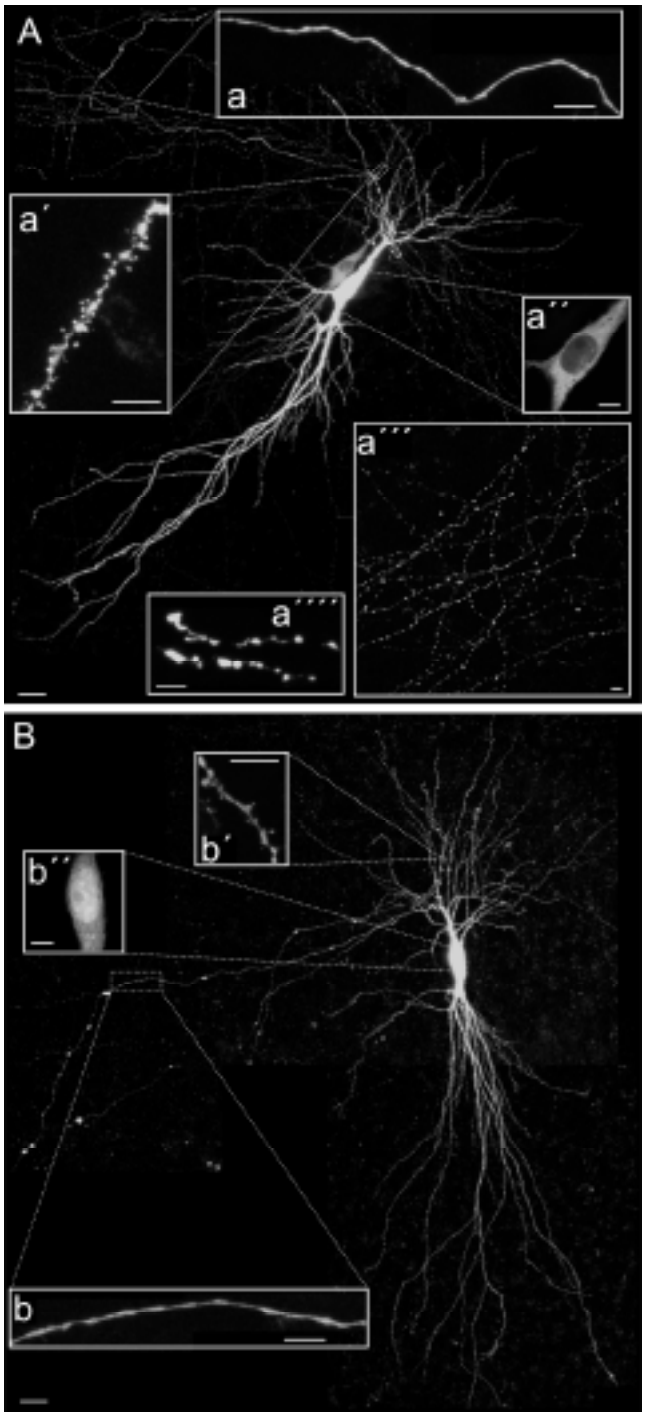

Fig. 3.9 Distribution of ChAT-GFP and GFP in CA3 hippocampal neurons in organotypic hippocampal brain slices after fixation. The plasmids *pJR38* (A) and *pEGFP* (B) were electroporated into pyramidal neurons of CA3. The slices were fixed 20 hours after electroporation and imaged by confocal microscopy. A) ChAT-GFP is present in the soma and translocates into axonal (a) and dendtritic processes (spines, a´) but is absent from the nucleus (a´´). B) GFP is also present in axonal (b) and dendtritic processes (b´) including the nucleus (b´´). Scale bars in A and B 20 µm, in a, a´, a´´ and b, b´, b´´5 µm.

and a´´). This indicates that a least some of the ChAT protein could be associated with synaptic vesicles of transport packets or presynaptic boutons. Again ChAT-GFP was absent from the nucleus (Figure 3.9a´´). The distribution in the soma was very similar to GFP (Figure 3.9B), which is known to be a cytoplasmic protein. In contrast to ChAT-GFP, GFP translocates into the nucleus (Figure 3.9b´´).

Generally fixation slightly affected the quality of the cellular morphology of the neurons in slice cultures as well as the fluorescence intensity of GFP. However, since the distributions of fluorescent proteins was analyzed before and after fixation, the results and the conclusions were reliable.

3.3 Transfection of individual neurons in organotypic hippocampal slice cultures by single-cell electroporation (SCE)

Experiments were performed to optimize conditions for the preparation and culture of organotypic hippocampal brain slices resulting in the following procedure: The hippocampus of P7 Wistar rats was dissected and sliced into 350 µm sections (see Section 2.2.3.3). Three hippocampal slices were placed on a Millicell-CM organotypic culture plate insert. The slices were maintained in the interphase of air and medium. Under these conditions the slices do not dry out, rather they remain covered by a film of medium and diffusion of medium contents through the membrane is sufficient for the survival of the cells in the cultured slice. After 5-7 days in the incubator the slices flattened from 350 µm to about 150 µm probably due to the elimination of injured cells. The stratum pyramidale from CA1 to CA3 broadened and finally contained 1-4 layers of cells (Figure 3.10A). These cells were healthy and viable as shown by labeling with dye or by GFP expression (Figure 3.11).

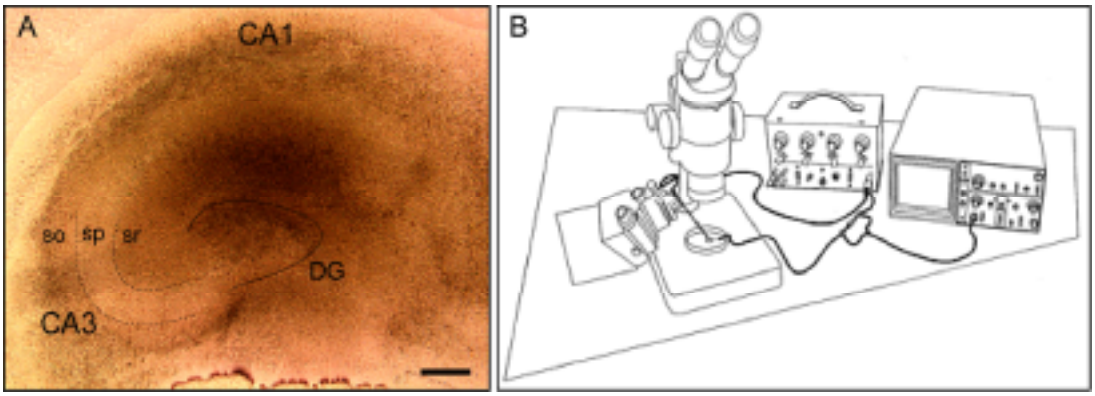

Fig. 3.10 Organotypic brain slice cultures used for single-cell electroporation. A) Organotypic hippocampal brain slice after 6 days in culture. CA1 to CA3 and dentate gyrus (DG) are clearly visible. The stratum pyramidale (sp) has broadened significantly during culturing. The image was taken with differential interference contrast (DIC). Scale bar 100 µm. B) Simplified setup for single-cell electroporation (SCE), taken from Haas et al. (2001). Instead of the dissection microscope a Zeiss Axioplan microscope with DIC optics, IR camera and 20x air objective with long working distance was used. For explanations see text.

Single-cell electroporation (SCE) and modification of published procedures

A single-cell electroporation unit has been set up for transfection of individual neurons. As illustrated in Figure 3.10B the Millicell-CM culture well containing the brain slices was placed in a culture dish containing culture medium on the stage of a Zeiss Axioplan microscope (instead of a dissection microscope). The cells were visualized by infrared differential interference contrast (IR-DIC) optics using a 20x air objective.

Micropipettes were pulled from capillary glass with filament, similar to conventional patch pipettes, with a tip diameter of about 1-2 µm and a resistance of 10-20 MΩ. The pipette was filled either with tetramethylrhodamine-dextrane or DNA solution and a thin silver wire was inserted into the pipette solution. The silver wire was connected to one terminal of a Grass SD9 stimulator. The stimulator produced square pulses mediating dye and DNA transfer across the cell membrane. A second wire connected to the other terminal as ground electrode was placed in the culture medium. Shape and amplitude of the currents passing through the pipette were monitored by measuring the voltage drop across a 100 kΩ resistor using an oscilloscope placed in

parallel with the circuit. The pipette mounted on a micromanipulator was inserted randomly into the CA3 area within the hippocampal slice.

At first the electroporation of tetramethylrhodamine-dextrane was applied to visualize the viability and morphology of hippocampal pyramidal cells and to test whether the shape of the pipette tip was good. As shown in Figure 3.11A several neurons were electroporated using a pipette filled with 2 mM tetramethylrhodamine-dextran. One to two 40 msec long square pulses of 15 V efficiently labeled numerous cells. The dye filled cells within 30 min diffusing throughout all neuritic processes. The efficiency of the electroporation of tetramethylrhodamine-dextrane was very high and estimated to be nearly 100 %. Since tetramethylrhodamine-dextrane is positively charged the pipette was connected to the anode and the ground electrode was connected to the cathode.

Compared to the small dye molecules it was much more difficult to electroporate plasmid DNA routinely with sufficient efficiency. After testing a range of pulse parameters three to five 1 sec long trains of 1 msec square pulses with an amplitude of 20 V delivered at 200 Hz, with a 6 sec interstimulus interval have initially been found to be the most efficient protocol for plasmid DNA transfer. Figure 3.11B shows two individual neurons electroporated with *pEGFP-C1* expressing GFP under control of the CMV promoter. The DNA concentration in the pipette was 1 µg/µl. Since DNA is negatively charged the pipette was connected to the cathode and the ground electrode was connected to the anode.

Next two plasmids were electroporated simultaneously, *pEGFP-C1* and *pDsRed2-C1*, each at a concentration of 0.5 µg/µl. Figure 3.11C and C´ shows a cell expressing both EGFP (in C) and DsRed (in C´). Both proteins diffused throughout the cell and labeled all neuritic processes. Often two neighboring cells were electroporated and expressed similar transgene levels. This occurred more often with larger pipette tip diameters.

The efficiency of electroporation using these conditions was about 5 % for GFP and DsRed. Generally, lower efficiencies resulted when electroporating larger plasmids encoding GFP fusion proteins and dropped below 1-2 %.

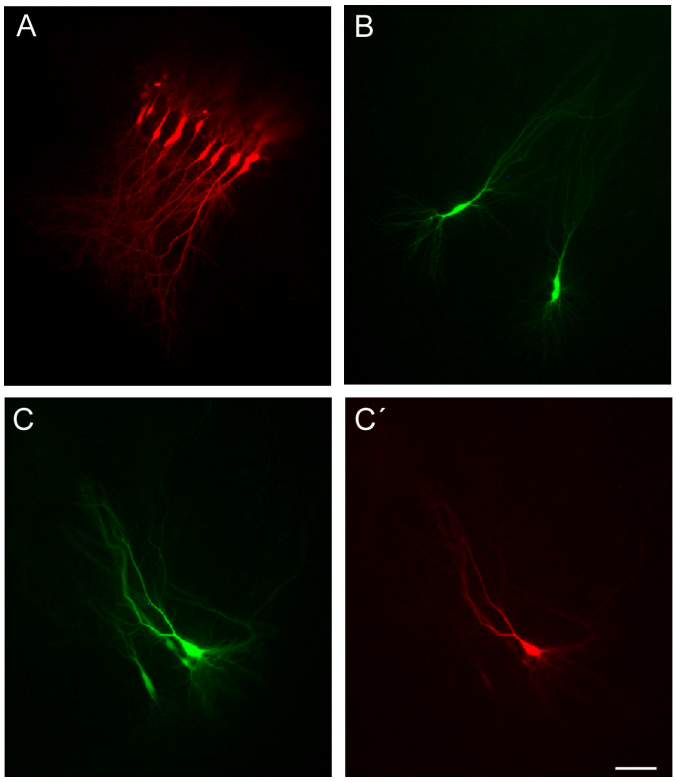

Fig. 3.11 Single-cell electroporation of CA3 pyramidal neurons in organotypic hippocampal brain slice cultures. A) Tetramethylrhodamine-dextrane labeled cells. B) Individual cells expressing EGFP. C, C´) Co-electroporated cells expressing EGFP (C) and DsRed (C´). Scale bar 100 µm.

To increase the efficiency of SCE it is essential to understand what happens during the pulse application and whether pulse application actually was correlated with plasmid DNA transfer through the cell membrane. Electroporation was therefore visualized using a setup equipped with a two-photon laser-scanning microscope (done by Thomas Nevian, Zellphysiologie, MPImF). The pipette was filled with the fluoresceine-conjugated oligonucleotide "JRscreenChATPCR" in a concentration of 1 µg/µl. Identical pulses as used before for electroporation of plasmid DNA were applied. Figure 3.12 shows a series of time-lapse images with an interval of 280 msec (overlays of the IR and fluorescence images). The experiments clearly revealed that the cell became sucessfully electroporated and was filled efficiently only when the pipette tip was directly in touch with the cell membrane at the soma of a hippocampal CA3 neuron (case in A). When the pipette tip was inserted randomly into stratum pyramidale

without touching a cell close to the soma the fluorescence would be found distributed in the intercellular space and no electroporation occured (case in B). Interestingly, a single train of pulses was sufficient to fill a cell while more than three trains were not beneficial for cell survival (data not shown).

These results demonstrate that direct contact between the pipette tip and the cell membrane is a very critical factor for sucessful electroporation and increased pulse frequencies as used before were too strong which in combination resulted in the low transfection efficiencies.

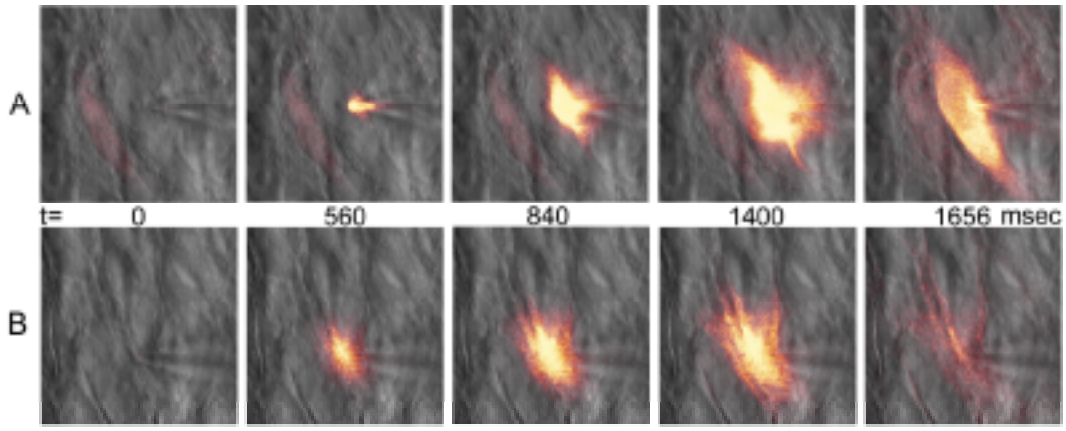

Fig. 3.12 Visualization of single-cell electroporation at real-time. A fluoresceine-conjugated oligonucleotide (1 µg/µl) was electroporated with 1 sec long trains of 1 msec square pulses of 20 V delivered at 200 Hz. Images were taken at 280 msec intervals. Overlays of the IR and fluorescence image are shown. A) The pipette tip is in touch with the cell membrane of a CA3 pyramidal neuron. B) The pipette tip is inserted randomly into stratum pyramidale.

SCE using improved electroporation conditions

On the basis of the directly observed electroporation the setup was modified accordingly. The Millicell insert with the cultured brain slice was placed into a customized perfusion chamber and was superfused with oxygenated physiological salt solution during the electroporation. This enabled to visualize the neurons by "Dodt" gradient contrast illumination and IR video microscopy using a 40x water immersion objective and a further 2x magnification.

Under this visual control the pipette tip could be guided very precisely and gently towards the membrane of an identified cell. It was directly seen whether the contacted cell was damaged or died during the pulse application. The pulses were generated by a Tetanizer-controlled isolated voltage stimulator, instead of the Grass

SD9 stimulator and appeared to be less stressful for the cells. Furthermore the voltage was reduced from 20 V to 10 V. The DNA was diluted to 33 ng/µl in mammalian saline and a back-pressure of about 3-4 mbar was applied to the pipette. This reduced clogging and ensured a constant flow out of the tip. By using these modifications the efficiency could be improved significantly to about 25-50 % for each slice but was still very variable. Usually 6-10 cells were electroporated in each slice. This took about 20 min under perfusion. As a result at least one cell was successfully transfected in each slice. So far several slices were cultured per Millicell insert. To reduce the time for slices being under perfusion only one slice was cultured per Millicell insert. Cells lying 25-40 µm beneath the surface were found to be optimal for electroporation. It has also been found that one 1 sec long train of pulses was usually sufficient for successful DNA transfer. Reduced stress resulted in an increased survival of the cells. After the electroporation the slice was transferred back into culture and maintained up to two weeks, the longest period tested, without contamination. The transfection efficiencies before and after the optimization of SCE are summerized in Table 3.2.

Tab. 3.2 Transfection efficiencies before and after optimization of single-cell electroporation (SCE).

optimization	rhodamine-dextrane	pEGFP-C1/pDsRed2-C1	GFP fusion constructs
before	~100 %	~5 % of 30 transfection attempts	~1-2 % of 30 transfection attempts
after	~100 %	25-50 % of 8 transfection attempts	25-50 % of 8 transfection attempts

The efficiency is determined by calculation of fluorescent cells versus electroporated cells (transfection attempt = electroporated cell). The slices were analyzed 20 hours after SCE.

3.4 Expression of presynaptic and postsynaptic marker proteins

With the optimized SCE setup, neurons were electroporated successfully with expression plasmids for synaptophysin-GFP and fusion constructs of AMPA type glutamate receptor subunit cDNAs, GluRA-GFP and GluRB-GFP. The distribution of the transgenically expressed proteins was analyzed in living cells by fluorescence microscopy (Figure 3.13) and after fixation of the brain slices by confocal microscopy (Figure 3.14).

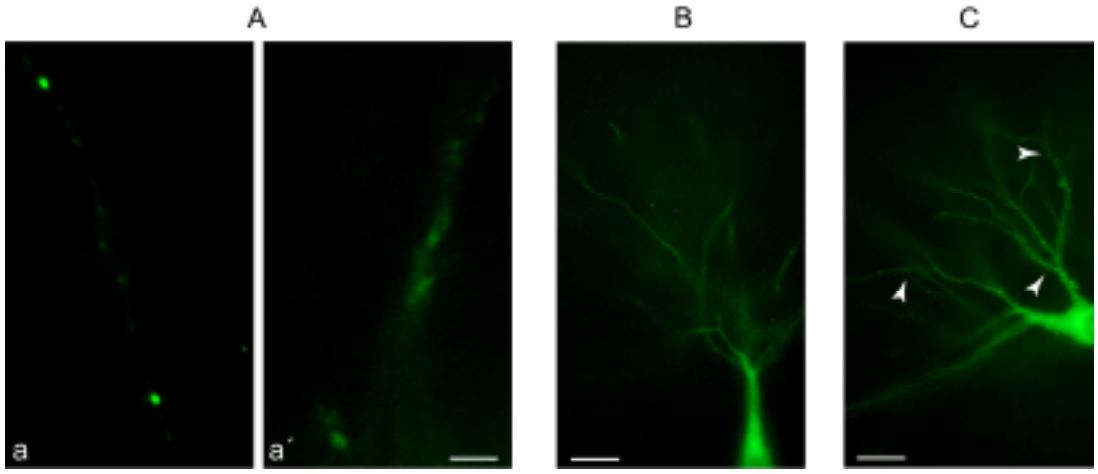

Fig. 3.13 Living hippocampal neurons in organotypic slice culture expressing presynaptic synaptophysin-GFP, postsynaptic GluRA-GFP or GluRB-GFP. Images were taken 20 hours after SCE by fluorescence microscopy. A) Synaptophysin-GFP had a punctate distribution and was accumulated in axonal projections in area CA1 (a) and was weakly present in dendrites (a´). B) GluRA-GFP was located in dendrites. The fluorescence appeared to be present in dendritic shafts and at the bottom of spines. C) GluRB-GFP was present in spines (some are indicated by arrowheads). Scale bar in A 5 µm, in B and C 20 µm.

The presynaptic marker protein synaptophysin-GFP translocated mainly into axonal processes and their varicosities (Figure 3.13a) and little was detected in dendrites (Figure 3.13b). It was transported to synaptic vesicles, probably associated with transport packets (Ahmari *et al*., 2000), which appears to be reflected by the characteristic punctate fluorescence (Figure 3.13a). A dense network of axonal processes was present in the CA1 area originating from one single cell in CA3 expressing synaptophysin-GFP (Figure 3.14a´). The punctate aggregates were about 1 µm in diameter as shown by the imaging of an axon terminal in CA1 (Figure 3.14a´´). The position of the fluorescent neuron and its projections is shown schematically in Figure 3.14a.

The expression of the postsynaptically localized AMPA receptor subunits GluRA and GluRB, each fused to GFP at the N-terminus, is shown before fixation in Figure 3.13 B,C and after fixation in Figure 3.14 B,C, respectively. Both proteins strongly labeled the dendritic tree of CA3 neurons. The fluorescence of GluRB-GFP in spines was brighter compared to the GluRA-GFP fluorescence. In higher magnification images the GluRB-GFP fusion protein appeared to be more concentrated in the heads of

dendritic spines (Figure 3.14b) than the GluRA-GFP which rather resided at the bottom of spines and the dendritic shafts (Figure 3.14c).

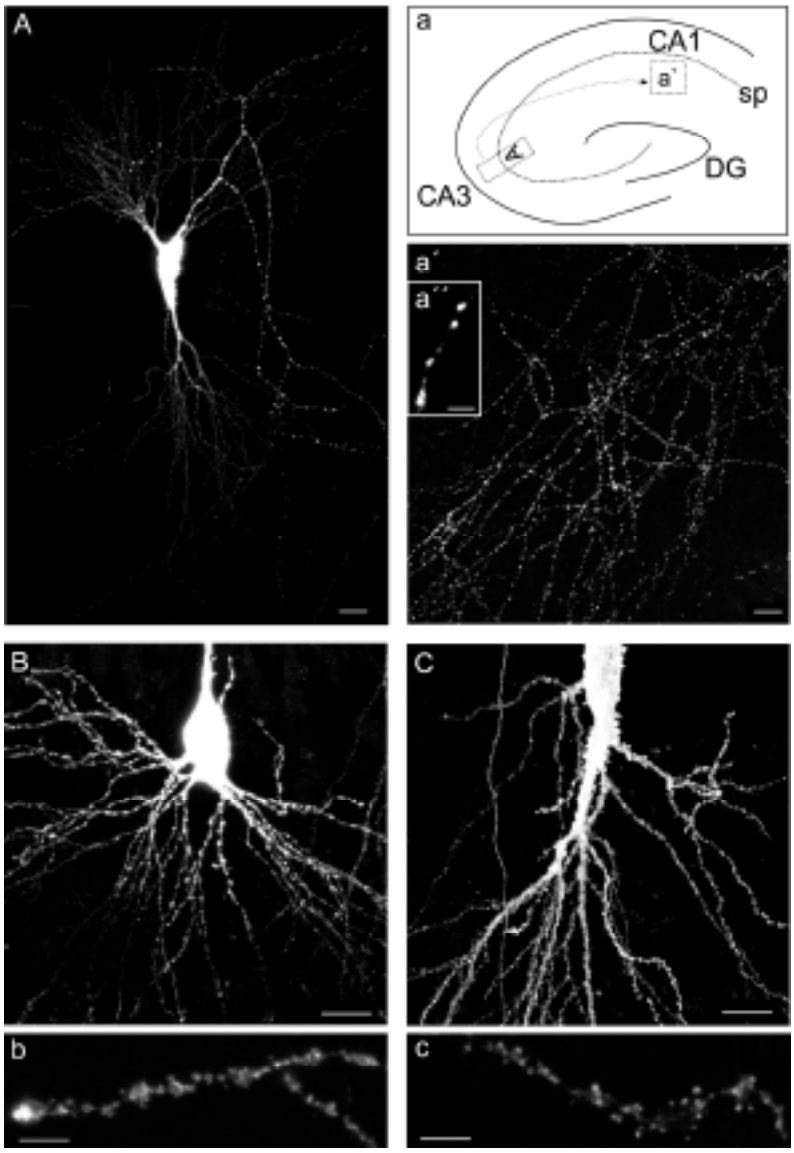

Fig. 3.14 Hippocampal neurons in organotypic slice culture expressing presynaptic synaptophysin-GFP, postsynaptic GluRA-GFP or GluRB-GFP. Slices were fixed 20 hours after SCE and images were taken by confocal microscopy.
A) Only one cell in CA3 expressed synaptophysin-GFP that was transported into axonal processes. The CA1 area was densely innervated by a network of axonal projections (a´). The position of the neuron and the path of the axonal projections are schematically illustrated (a). sp, stratum pyramidale; DG, dentate gyrus. Higher magnification image of the fluorescent puncta in axon terminals (a´´). B) GluRA-GFP is located in dendrites. The fluorescence appears concentrated in dendritic shafts and at the bottom of spines. (b) C) GluRB-GFP is present in spine heads (c). Scale bars in A, a´, a´´ and B 20 µm, in B and C 10 µm, in b and c 5 µm.

3.5 Generation of ChAT-GFP and ChAT-loxP targeted mouse E14 stem cell clones

The ChAT-GFP targeting vector (*pJR48,* Figure 3.2) was linearized by XhoI digestion. Embryonic (E14-1) stem cells were electroporated with the targeting vector and subsequently the cells were selected for G418 resistance. 800 resistant clones were isolated and maintained for the preparation of genomic DNA. Positive clones, which integrated the modified sequences by homologous recombination, were identified by PCR screening using the primer pair "pgk-Prom (R)/JRPCRscreen3" as explained in Figure 3.15.

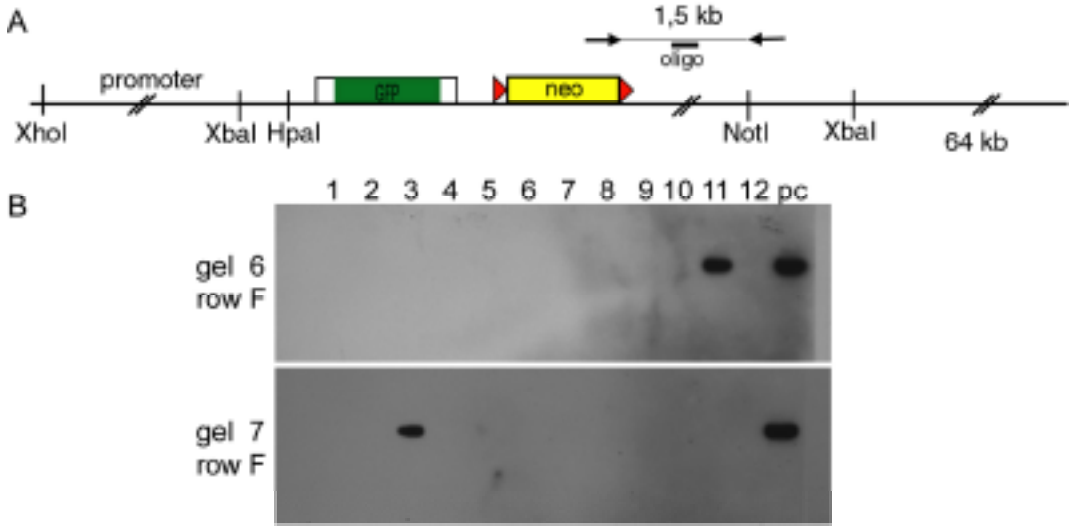

Fig. 3.15 PCR screen of ChAT-GFP targeted ES cell clones. A) The forward primer binding at the 3´ site of the neo^r sequence and the reverse primer binding outside of the targeting vector sequence generates a 1,5 kb PCR fragment which was detected with a fluorescently labeled olidonucleotide. B) ES cell clones 6F11 (lane 11) and 7F3 (lane 3) showed positive signals in this Southern blot developed using the ECL system. pc, positive control.

A 1.5 kb fragment amplified by PCR with a forward primer which binds at the 3´site of the neo^r cassette and a reverse primer binding 10 bp downstream the NotI site outside the vector sequence was detected with a fluoresceine-labeled oligonucleotide probe indicating the proper integration of the transgene into the ChAT genomic locus (Figure 3.15B). Here the clones 6F11 and 7F3 were identified and further characterized by genomic Southern blot hybridization using a α-^{32}P-dCTP labeled 500 bp genomic

fragment flanking the NotI site as illustrated in Figure 3.16A. As shown, the genomic fragment was outside the targeting vector sequence and served as a specific probe binding the HpaI- and XbaI- wildtype fragments as well as the recombined fragments. The HpaI digestion of wildtype genomic DNA showed an approximately 4.5 kb band while the proper integration of GFP and loxP-neo^r-loxP resulted in a shift to approximately 7.2 kb. The XbaI digestion showed a 3.4 kb band for the wildtype which was reduced in the targeted locus to 2.4 kb due to an additional XbaI site within the neo^r sequence. Only clone 6F11 was confirmed to be correctly targeted (Figure 3.16B).

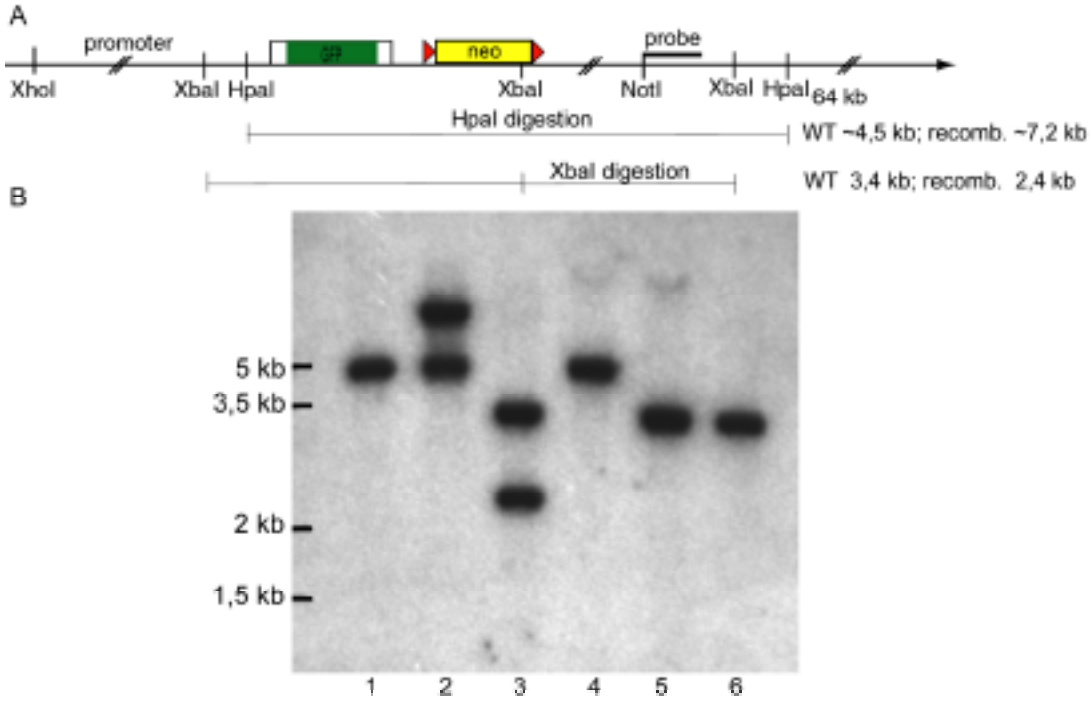

Fig. 3.16 Genomic Southern blot hybridization analysis of identified ChAT-GFP targeted ES cell clones. A) Digestion of genomic DNA with HpaI generates a wildtype fragment of 4.5 kb that is shifted to 7.2 kb when GFP and neo is properly inserted. Digestion with XbaI generates a wildtype fragment of 3.4 kb that is reduced to 2.4 kb due to an additional XbaI site in the neo sequence. B) Wildtype HpaI fragment (lane 1), targeted HpaI fragment of clone 6F11 (lane 2), targeted XbaI fragment of clone 6F11 (lane 3), wildtype HpaI fragment of clone 7F3 (lane 4), wildtype XbaI fragment of clone 7F3 (lane 5), wildtype XbaI fragment (lane 6). Only clone 6F11 is properly targeted.

Clone ChAT-GFP-6F11 with genotype ChAT$^{(GFP/+)}$ was used to produce "knock-in" animals (Transgene Lab, ZMBH, Universität Heidelberg). Blastozysts were injected with ChAT$^{(GFP/+)}$ ES cells and transferred into pseudo pregnant females. The offspring

comprised 14 animals of 20-70 % chimerism. Male animals with chimerism over 50 % will be bred with C57Bl/6 females to obtain mice heterozygous for the modified allele (ChAT$^{(GFP/+)}$ mice).

Similarly ChAT-loxP targeted ES cells were generated (Figure 17A) and among 800 G418 resistant ES cell clones one clone, 6G12 (genotype ChAT$^{(loxP/+)}$), was identified by PCR screening and found to be correctly targeted for loxP sites (Figure 3.17B).

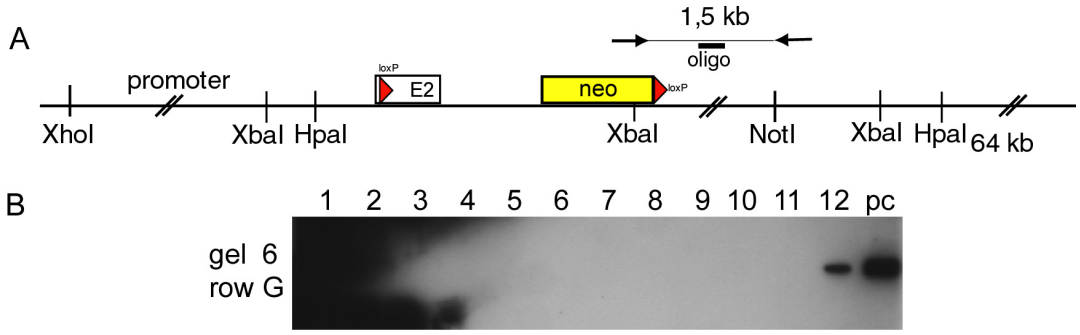

Fig. 3.17 PCR screen of ChAT-loxP targeted ES cell clones. A) The forward primer binding at the 3´ site of the neo sequence and the reverse primer binding outside the targeting vector sequence generates a 1.5 kb PCR fragment which was detected with a fluorescently labeled olidonucleotide. B) ES cell clone 6G12 (lane 12) showed a positive signal in this Southern blot developed using the ECL system. pc, positive control

Genomic Southern blot hybridization confirmed that the gene locus was modified as expected (Figure 3.18). In contrast to the ChAT-GFP locus the HpaI fragment shifted only to about 6.5 kb instead of 7.2 kb corresponding to the 700 bp of the GFP cDNA. The clone ChAT-loxP-6G12 will also be transferred into blastocysts to generate ChAT$^{(loxP/loxP)}$ targeted mice.

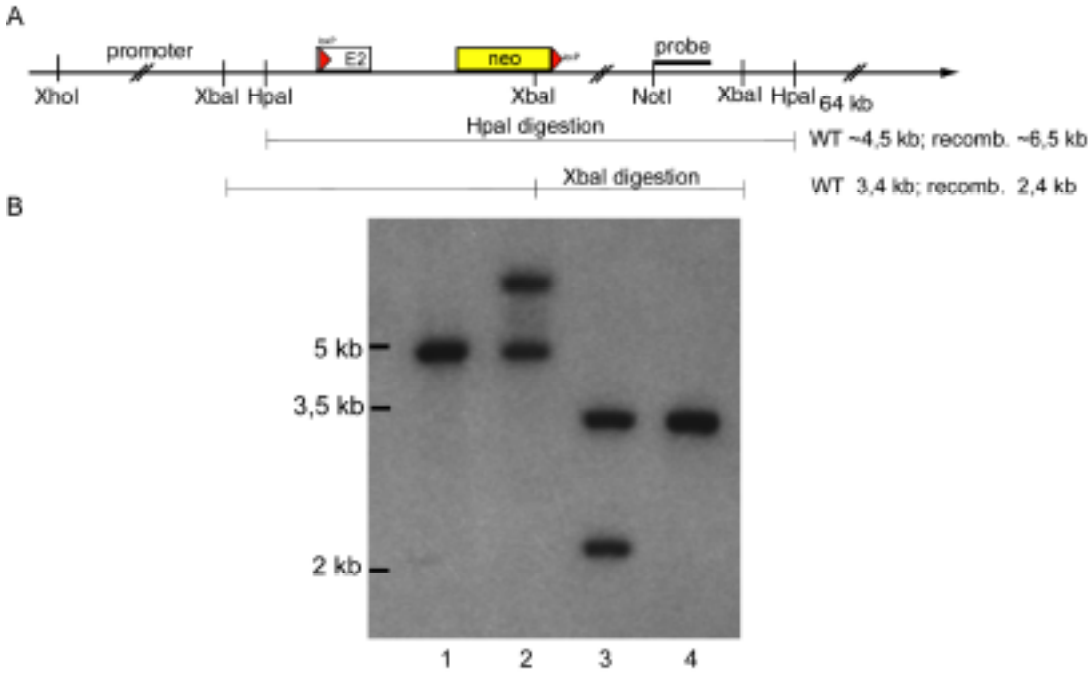

Fig. 3.18 Genomic Southern blot hybridization of identified ChAT-loxP targeted ES cell clones. A) Digestion of genomic DNA with HpaI generated a wildtype fragment of 4.5 kb that is shifted to 6.5 kb when the loxP site and neo is properly inserted. Digestion with XbaI generated a wildtype fragment of 3.4 kb that is shifted to 2.4 kb due to an additional XbaI site in the neo sequence. B) Wildtype HpaI fragment (lane 1), targeted HpaI fragment of clone 6G12 (lane 2), targeted XbaI fragment of clone 6G12 (lane 3), wildtype XbaI fragment (lane 4).

Taken together the frequency of the recombination of the ChAT gene in ES cells by homologous recombination was 1/800 (0.125 %) for both ChAT-GFP as well as ChAT-loxP.

To confirm that the sequence of the genomic locus adjacent to exon 2 was intact in both targeted ES cell clones, fragments comprising exon 2 were amplified by PCR with the primer pair "JR18.seqBsaBI/pgk-Prom(R)", cloned into the *pCR-BluntII-TOPO* vector and verified by DNA sequence analysis.